Barrier Properties of Blends Based on Liquid Crystalline Polymers and Poly(ethylene terephthalate)

G. Flodberg[a]; L. Höjvall[a]; M. S. Hedenqvist[b]; E. R. Sadiku[c]; U. W. Gedde[b]

[a] The Foundation Packforsk - The Institute for Packaging and Distribution, Kista [b] Department of Polymer Technology, Royal Institute of Technology, Stockholm, Sweden [c] Dept. of Chemistry, Federal University of Technology, Minna, Nigeria

PLEASE SCROLL DOWN FOR ARTICLE

Barrier Properties of Blends Based on Liquid Crystalline Polymers and Poly(ethylene terephthalate)

G. FLODBERG[a], L. HÖJVALL[a], M. S. HEDENQVIST[b],
E. R. SADIKU[c] and U. W. GEDDE[b,*]

[a] *The Foundation Packforsk — The Institute for Packaging and Distribution,*
P. O. Box 9, SE-164 93 Kista; [b] *Royal Institute of Technology,*
Department of Polymer Technology, SE-100 44 Stockholm, Sweden;
[c] *Federal University of Technology, Dept. of Chemistry, P.M.B 65, Minna, Nigeria*

Blends of poly(ethylene terephthalate) (PETP) and two different thermotropic liquid crystalline (LC) polymers of the Vectra-type were prepared by melt mixing. Oxygen and water vapor permeability, light transmission and welding properties were measured on compression-molded and film-blown specimens. SEM showed that the LC polymers were the disperse phase with a good phase adhesion to the PETP matrix in the majority of the compression-molded blends. The 50/50 blend based on the low melting point LC polymer showed possibly a continuous LC polymer phase. The film-blown specimens showed LC polymer spheres at low LC polymer content. Above a certain LC polymer content (10–30% LC polymer), fibrous and ellipsoidal LC polymer particles was the dominant morphological feature of the blends. Density measurements showed that the void content in the blends was low. The compression-molded blends based on the high melting point LC polymer showed permeabilities conforming to the Maxwell equation assuming low permeability (LC polymer) spheres in a high permeability (PETP) matrix. The compression-molded blends based on the low melting point Vectra showed lower permeabilities than predicted by the Maxwell equation, particularly at high LC polymer content. The film-blown blends showed extensive scattering in the permeability data. The blend with 30% low melting LC polymer exhibited a 96% lower oxygen permeability than PETP. This was due to a reduction in both oxygen diffusivity and solubility. Ellipsoidal and fibrous LC polymer particles increased the diffusional path and lowered the diffusivity. The transparency of the compression-molded samples was lost already at 1% LCP. The blends showed welding properties superior to those of PETP.

Keywords: Blends; Poly(ethylene terephthalate); Liquid crystalline polymers; Barrier properties; Morphology

*Corresponding author.

157

INTRODUCTION

The use of poly(ethylene terephthalate) (PETP) in packaging has increased during recent years due to the recent reduction in price to a level close to that of commodity polymers like polyethylene (PE). PETP has better gas barrier properties and better optical clarity than PE, which makes it suitable as a packaging material for carbohydrate beverages [1]. The barrier properties of PETP are nevertheless insufficient to avoid the sorption of aroma compounds and to cause odor changes in *e.g.*, mineral water, which has been stored in refilled bottles [2]. Therefore attention has been given to poly(ethylene naphthalate) as a replacement for PETP. Due to its low chain flexibility, poly(ethylene naphthalate) has an oxygen permeability four times lower than that of PETP [3]. The price per barrier is currently (1999) however twice that of PETP [3]. An alternative approach is to increase the barrier properties of PETP by laminating it with a high barrier material such as a liquid crystalline (LC) polymer. This method makes high demands on the adhesion between the two layers, and the lamination procedure may be complicated. Material recycling may also be difficult to handle due to the laminated structure. A third possibility is to blend PETP with LC polymers. Extrusion can be followed by stretch-blow molding to manufacture bottles [3]. During stretch-blow molding, the blend is biaxially stretched and this results in elongated LCP particles. It was possible to decrease the oxygen permeability of such blends by 75–92% at a LC polymer content of 30% by this method. A fourth possibility is extrusion preblending of PETP and LCP followed by compression molding or film blowing. In a recent study, Wiberg *et al.* [4] obtained good barrier properties for an LC polymer/poly(ether sulfone) blend even at very low LC polymer content by pre-extrusion followed by compression molding. The excellent barrier properties of this blend were due to the formation of a continuous surface layer of LCP. Baird and Wilkes [5] reported on an LC polymer-rich surface skin in injection-molded LC polymer/PETP blends. Flodberg *et al.* [6] obtained a similar morphology in blends of Vectra and PE.

This paper reports on the barrier properties of extrusion-blended PETP-LC polymer blends which were subsequently compression-molded or film-blown. Oxygen and water vapor permeabilities were

measured and the obtained results were explained on the basis of blend morphology and the rheological properties of the constituents. The blends were also characterized with respect to other relevant properties for packaging, *i.e.*, seal strength and transparency.

EXPERIMENTAL

Materials

The LC polymers studied were unfilled Vectra A950 – a copolyester consisting of 73 mol% *p*-hydroxybenzoic acid and 27 mol% 2-hydroxy-6-naphthoic acid with a melting point of approximately 280°C and an experimental Vectra grade (RD501) with a low melting temperature (220°C). Ticona AG, Germany kindly supplied both these LC polymers denoted A950 and RD501. The density of both polymers was 1400 kg/m^3. The poly(ethylene terephthalate) (PETP), Kodapak PET copolyester 9921, Eastman Chemical Company, USA had a room temperature density of 1330 kg/m^3.

Sample Preparation

The LC polymers were dried for 48 h in an oven at 120°C before the blending. Pelletized blends of LC polymer and PETP were produced in a Brabender Twin Screw Compounder DSK 35/9 mounted to a Plasti-Corder drive unit and an interface PL 2000, extruder type (± 35/9D). The temperature gradient was set between 290°C and 270°C for A950/PETP. The die temperature was 270°C and the screw speed was 25 rpm. For RD501/PETP, an extruder gradient between 250°C and 245°C was used. The die temperature ranged from 236°C to 240°C. The screw speed was set from 20 to 40 rpm. A Brabender pelletizing unit was used for the strands but for the blendings containing 30 to 50% of LC polymer a Moretto mill ML 18/10 pelletizer equipment was also used due to the stiffness of the strands.

Films were produced by film blowing using the same extruder equipped with a film blowing unit. The granules were pre-dried 8 – 12 h in a Piovan T10 IX DS 403 drier connected to the extruder. Different temperature gradients for A950/PETP blends were used in the range from 300°C to 240°C. The die temperature was set at

240°C to 260°C. The screw speed was 5 rpm and the take-up speed was 6 to 9.4 m/min. For RD501/PETP blends the temperature gradient was 255°C to 260°C and the die temperature was 255°C. The screw speed ranged from 10 to 50 rpm (50/50 blend). The take-up speed was set from 0.9 (50/50 blend) to 9 m/min.

Thin compression molded films were made in a Schwabenthan Polystat 400S machine at 310°C for A950/PETP and 300°C for RD501/PETP for 15 min. followed by quenching in liquid nitrogen to avoid crystallization of PETP. This time of 15 min. enabled production of films with a minimum concentration of visible holes. Before compression molding the pelletized material and also Vectra A950 and Vectra RD501 were pre-dried for 65 h at 150°C and 0 atm. The sample size for film making was 1.5 g and the pellets were spread out in a circular formation with a diameter of about 30 mm on a release film made of 0.15 mm thick PTFE coated glass-fiber cloth (Fluortek AB, Sweden). The pressure applied was 25 bar and the thickness of the films produced ranged from 61 μm to 137 μm. Further details about the compression molding procedure and its implication on the film quality is reported in another paper [7].

Measurements

Scanning Electron Microscopy

Scanning electron microscopy was performed on specimens cracked at the temperature of liquid nitrogen or during Instron tensile tests at 23 ± 2°C. The samples were gold/palladium-coated and examined in a JEOL JSM-5400.

Differential Scanning Calorimetry (DSC)

Thermograms of 5–10 mg samples were recorded between −30°C and 350°C at a heating rate of 10°C/min in a Perkin–Elmer DSC-7 and a Mettler DSC 820.

X-ray Scattering

X-ray scattering patterns were recorded with a Statton camera using the Ni-filtered Cu-K_α radiation from a Phillips PW 1830 generator.

Shear-viscosity

The shear viscosity was measured using a "plate-to-plate" Stress Tech Rheometer. The plate diameter was either 20 mm or 30 mm and the plate-to-plate gap was 0.2 mm. The rheometer was equipped with an "elevated temperature cell" coupled with an oven which ensured constant temperature during each measurement. The sample cell was flushed with nitrogen gas to avoid oxidation of the polymer studied.

UV-VIS Spectroscopy

A Hewlett-Packard 8415A Diode Array spectrometer was used to measure the light absorption.

Oxygen Permeability Measurements

The permeability of the films to oxygen was obtained at 23°C at 0% RH in a Mocon OX-TRAN TWIN device. The samples with a thickness of $17-137\,\mu m$ were mounted in an isolated diffusion cell and were subsequently flushed with flowing nitrogen to remove sorbed oxygen from the specimens. The specimens had a circular exposure surface area of $4.9\,cm^2$ achieved by covering a part of the sample with a tight aluminum foil. One side of the sample was initially exposed to flowing oxygen (1% hydrogen) at atmospheric pressure while the oxygen pressure was zero on the other side of the specimens. The flow rate (Q) through the specimen was measured during the transient period until the steady state flow rate (Q_∞) was obtained. The permeability of the films to oxygen, P, was obtained according to:

$$P = \frac{Q_\infty l}{p} \tag{1}$$

where l is the thickness of the specimen and p is the partial pressure of oxygen on the high oxygen pressure side of the specimen. The mean value of bias, both positive and negative was 6.7% for the oxygen permeability measurements. This bias was calculated from results obtained from eight round robin tests.

Water-vapor Transmission Rate Measurements

The water vapor transmission rate was measured in a Mocon Permatran-W Twin at 23°C and 100% RH, according to ASTM F 1249–90. The specimens with thicknesses ranging between 17 μm and 137 μm, depending on the processing method used, were mounted in an isolated diffusion cell containing deionized water. The specimen, sandwiched tightly, between two aluminum foils, had a circular exposure surface area of 4.9 cm^2. The mean value of bias, both positive and negative was 9.9% for the water vapor permeability measurements. This bias was calculated from results obtained from eight round robin tests.

Density Measurements

The densities of the materials were obtained using the Avogadro principle, *i.e.*, by comparing the weights of the samples in air and in ethanol. The density kit provided by Mettler–Toledo was used for this purpose together with a AT 261 balance with resolution 10^{-5} g.

Seal Strength Measurements

The seal strength of welded films (0.01–0.06 mm thick films, welded in a Multivac A300 during 10 heat pulses, duration of pulse: 2 s) was determined using an Alwetron TCT10 tensile testing machine at 23 ± 2°C, 50% RH and 100 mm/min elongation rate. The gauge length was 40 mm.

RESULTS AND DISCUSSION

Blend Morphology

SEM showed that PETP was always the discrete phase in the compression-molded blend samples (Fig. 1). The PETP component was, in contrast to the case of the polyethylene (PE) phase in the LC polymer/PE blends [6], spherical in all the blends with one possible exception. The PETP/RD501 50/50 blend showed a surface pattern in which it was difficult to make a clear distinction between the two
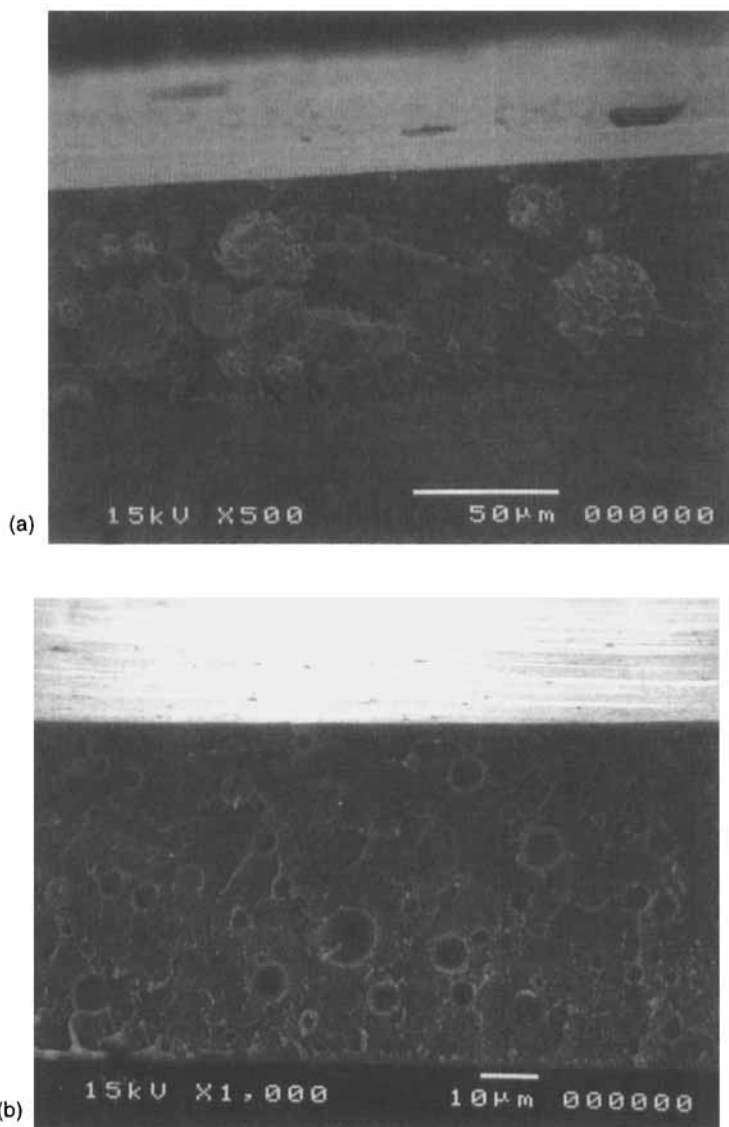
FIGURE 1 Scanning electron micrographs of fracture surfaces of compression-molded specimens: (a) A950/PETP 30/70; (b) RD501/PETP 20/80.

components. The "hairy" surface of the spherical LC polymer particles evident in the micrographs of Figure 1 indicated that there was some adhesion between the phases.

Figure 2 shows that the average diameter of the LC polymer particles increased only moderately with increasing LC polymer content and that it was significantly lower than that of the LC polymer particles in the LC polymer/PE blends [6].

Spherical LC polymers particles were observed in the film-blown blend samples containing only small amounts of LC polymer (Fig. 3). Blends containing ≥ 10% LCP in the A950 blend series and ≥ 30% in the RD501 blends contained fibrous and ellipsoidal LC polymer particles (Fig. 3). In the PE blends, similar transitions occurred at LC polymer contents of 20% for the A950-series and 5% for the RD501 blend series [6]. Once fibers were present, ellipsoidal particles were also observed. The fraction of LC polymer in fibrous or ellipsoidal particles increased with increasing LC polymer content. Figure 4 shows that the LC polymer particles (spheres, ellipsoids and fibers) were smaller than 5 µm, which is considerably smaller than the LC polymer particles present in the LC polymer/PE blends [6].
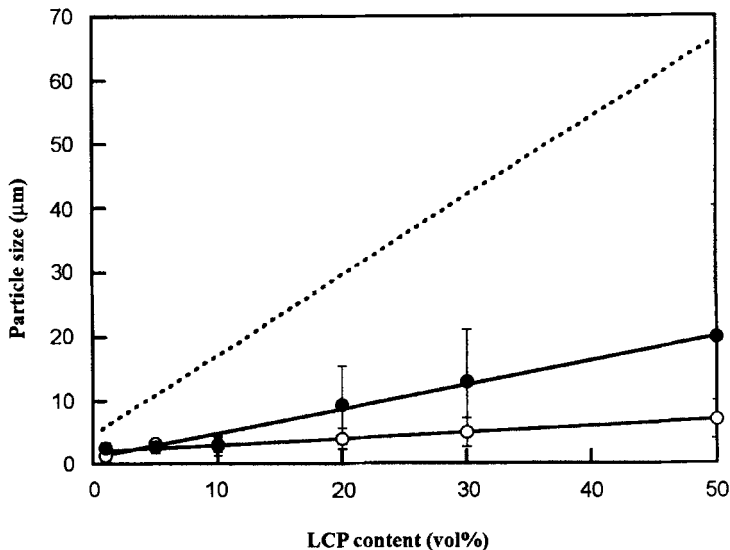
FIGURE 2 The size of LC polymer particles in compression-molded specimens (•: A950, ○: RD501) as a function of LC polymer content. The bars indicate the range of particle sizes. The dashed line indicates the average particle sizes for the LC polymer/PE blends [6].
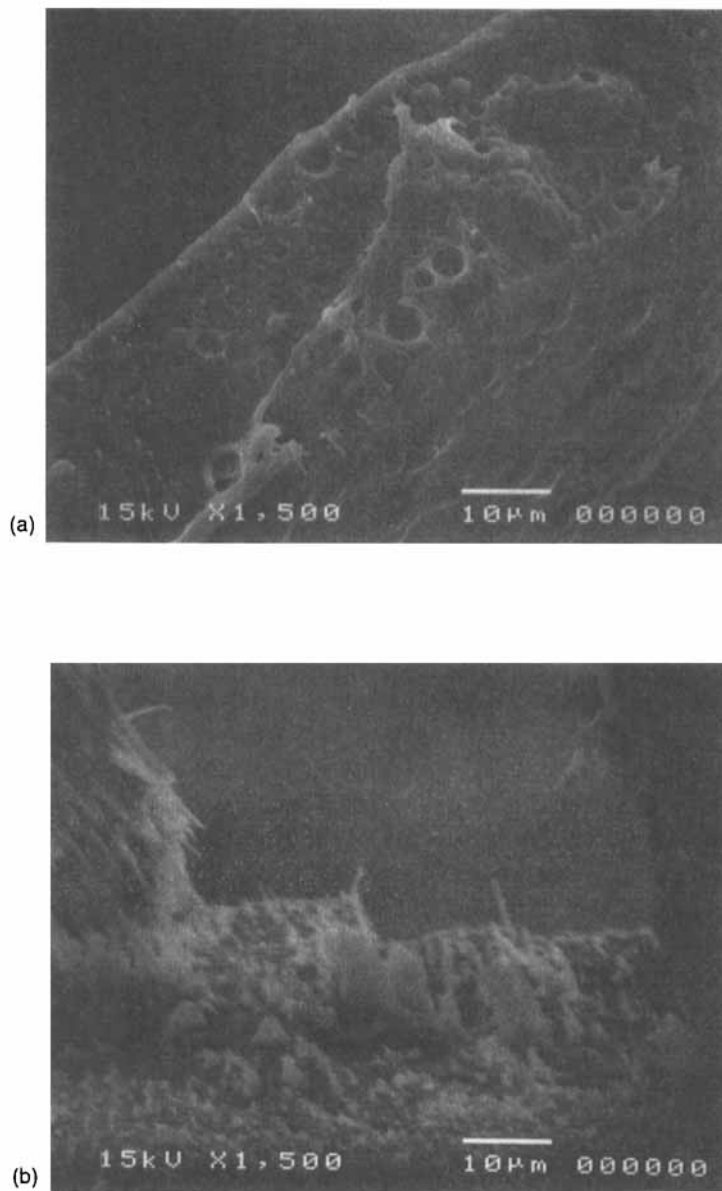
FIGURE 3 Scanning electron micrographs of fracture surfaces of film-blown specimens: (a) A950/PETP 5/95; (b) RD501/PETP 30/70.
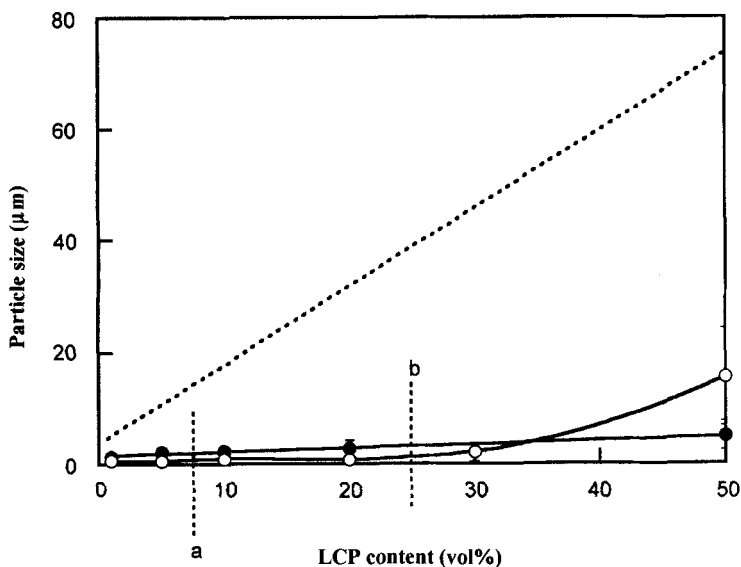
FIGURE 4 The size of LC polymer particles in film-blown specimens (•: A950, ○: RD501) as a function of LC polymer content. The bars indicate the range of particle sizes. The transitions from spherical particles to fibrous and ellipsoidal particles are indicated by the dotted lines (a: A950; b: RD501). The broken line indicates the average LC polymer particle sizes of film-blown LC/PE polymer blends [6].

The reason why PETP was always the continuous phase in the blends can be found in the rheological properties of the constituents of the blends. The shear viscosity of the PETP grade used was lower than the shear viscosity of A950 at shear rates lower than $\sim 1000\,\mathrm{s}^{-1}$ (Fig. 5a). RD501 exhibited a higher shear viscosity than PETP at 290 and 300°C and shear rates less than $20\,\mathrm{s}^{-1}$, whereas at 250 and 260°C the shear viscosities of RD501 and PETP were about the same (within 20%) at shear rates $\leq 100\,\mathrm{s}^{-1}$ (Fig. 5b). Phase inversion in polymer blends can be predicted from the expression proposed by Paul and Barlow [8]:

$$v_{\mathrm{LCP}}^{\mathrm{inv}} = \frac{1}{1 + (\eta_{\mathrm{PETP}}(\dot{\gamma})/\eta_{\mathrm{LCP}}(\dot{\gamma}))} \tag{2}$$

where $v_{\mathrm{LCP}}^{\mathrm{inv}}$ is the volume content of LC polymer at which phase inversion occurs, and $\eta_{\mathrm{PETP}}(\dot{\gamma})$ and $\eta_{\mathrm{LCP}}(\dot{\gamma})$ are the shear viscosities of the constituents.
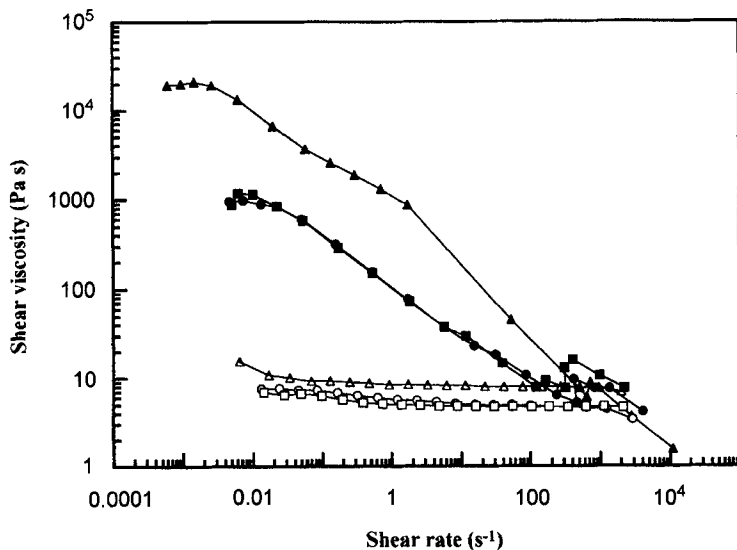
FIGURE 5a   Shear viscosity as a function of shear rate for A950 at 310°C (●), 300°C
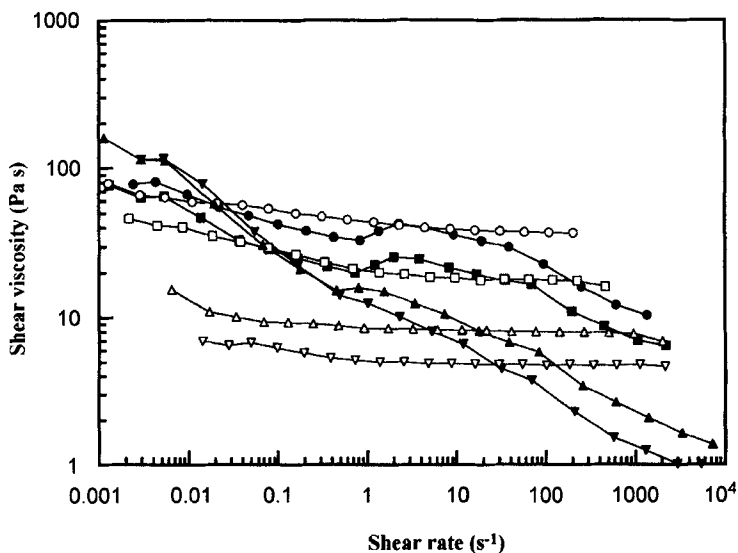(■), 290°C (▲) and PETP at 310°C (○), 300°C (□), 290°C (△).

FIGURE 5b   Shear viscosity as a function of shear rate for RD501 at 250°C (●), 260°C
(■), 290°C (▲), 300°C (▼) and PETP at 250°C (○), 260°C (□), 290°C (△), 300°C (▽).

Equation (2) predicts that the LC polymer should be the dispersed phase in the A950/PETP blend series at blend compositions well above 50% LC polymer. Phase inversion in the RD501 blend series should appear according to Eq. (2) at 45–50% LC polymer (compression molding) and 35–50% LC polymer (film blowing; shear rates = $1-100\,s^{-1}$). Hence, a continuous LC polymer phase was according to Eq. (2) possible only in the case of the RD501/PETP (50/50) blend. SEM neither confirmed nor rejected this prediction. Similar droplet-matrix morphologies have been reported for LCP/PETP single-screw-extruded blends which were quenched on a chill roll immediately after passing the slit die [9].

Due to the small difference in density between the LC polymers and PETP, the scatter in density data for the different blends was significant but no systematic deviation from a linear trend between the densities of the constituents was observed. It may thus be concluded that the void content in the blends was small. It is believed that the low void content was due to the good adhesion between PETP and the LC polymers and to the small difference in thermal contraction. Calculation based on data of Refs. [10] and [11] suggested a 9% greater shrinkage of PETP on cooling from the melt to room temperature.

Another potentially important factor for the permeability is the degree of orientation of the continuous PETP phase in the film-blown specimens. The macroscopic effective draw ratio (λ_{eff}) of the film-blown specimens was calculated as:

$$\lambda_{eff} = \frac{1}{2}\left(\frac{\phi_f}{\phi_d} + \frac{\phi_d}{\phi_f}\frac{t_d}{t_f}\right) \tag{3}$$

where the first term is the elongation in the transverse direction measured as the ratio of the diameter of the blown film (ϕ_f) to the film diameter at the die (ϕ_d). The second term is associated with the elongation in the machine direction, and is calculated from the thickness of the film at the die (t_d) and the thickness of the blown film (t_f) assuming constant volume.

Both the oxygen and the water vapor permeabilities showed only small variations in spite of very substantial changes in effective draw ratio. The very large oxygen permeability of one of the samples (film-blown λ_{eff} = 3.65) seems unrealistic (Tab. I).

TABLE I   Permeability data for PETP specimens

Process	λ_{eff}	$w_c{}^a$	$P_{O_2}{}^b$	$P_{H_2O}{}^c$
Compression molding	1.0	0.00	$6.3 \cdot 10^{-10}$	1.9
Film blowing	3.7	0.05	$27 \cdot 10^{-10}$	2.4
Film blowing	8.2	0.09	$6.6 \cdot 10^{-10}$	2.1

[a] Mass crystallinity by DSC.
[b] Permeability in cm^3 (STP) cm/(cm^2 s atm).
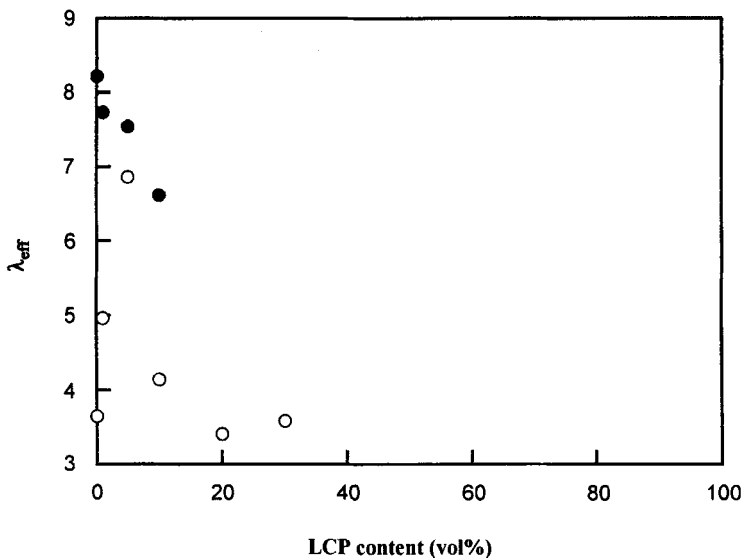[c] Permeability in g mm/(m^2 day atm).

FIGURE 6   Effective biaxial draw ratio (calculated from Eq. (2)) for film-blown specimens: A950/PETP (●); RD501/PETP (○).

The diffuse X-ray diffraction pattern of compression-molded and film-blown PETP indicated that the material was mostly amorphous. In addition, the uniform diffraction pattern, sampled normal to the film surface, of the film-blown specimen indicated that the material was biaxially stretched to approximately the same levels in the parallel and perpendicular directions. DSC indicated that the PETP in the compression-molded samples was fully amorphous (Tab. I). The PETP component in the film-blown samples showed according to DSC crystallinities in the range of 5 to 9% (Tab. I).

Figure 6 shows the effective draw ratio of the film-blown blend specimens as a function of the LC polymer content. The effective

draw ratio decreased strongly with increasing LC polymer content. However, the small differences in water vapor permeability found for PETP stretched to different draw ratios (Tab. I) suggest that the observed variation in effective draw ratio (*i.e.*, of chain orientation in the PETP) in the film-blown blends should be of only secondary importance for the transport properties.

Transport Properties

Figures 7 and 8 show that the oxygen and water vapor permeabilities decreased monotonously with increasing LC polymer content for the compression-molded blends. The data followed a slightly non-linear, concave curve with only a few data points (RD501/PETP blends with 30 and 50% LC polymer) that clearly deviated from the general trend. The blend with 50% RD501 showed permeabilities that were only 15 to 30% of the value prescribed by the general trend.

A previous paper [6] reported that the decrease in oxygen permeability of compression-molded specimens of LCP/PE blends with
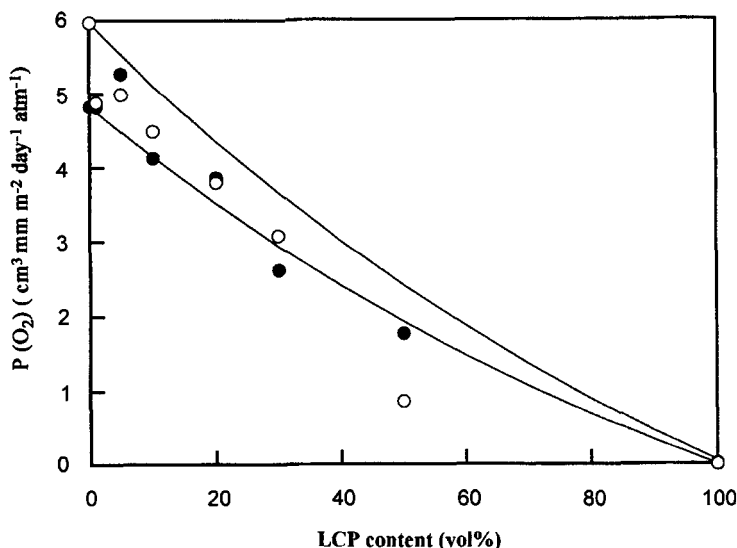

FIGURE 7   Oxygen permeability of compression molded A950/PETP (●) and RD501/PETP (○) as a function of LC polymer content. The continuous lines are predicted values based on Eq. (4).
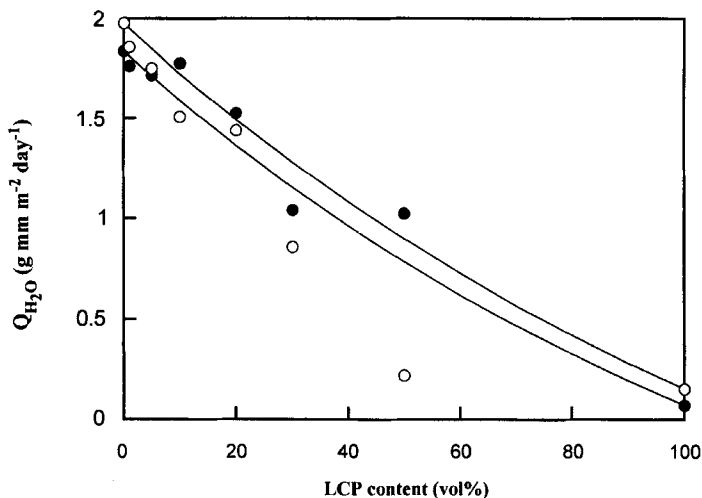
FIGURE 8 Water vapor transmission rates in compression molded A950/PETP (●) and RD501/PETP (O) as a function of LC polymer content. The continuous lines are predicted values based on Eq. (4).

increasing LC polymer content followed the Maxwell equation, which predicts the permeability of a system with discrete low permeability spheres contained in a high permeability matrix:

$$P = P_m \left[1 + \frac{3(1 - v_m)}{((p + 2)/(p - 1)) - (1 - v_m)} \right] \qquad (4)$$

where p is the ratio of the permeabilities of the discrete to the matrix phases, P_m is the permeability of the matrix phase and v_m is the volume fraction of the matrix phase. Further details about the Maxwell equation can be found in Refs. [12] and [13].

The experimental data obtained for the A950/PETP blend series showed only very small deviations from Eq. (4) (Figs. 7 and 8). The permeability of the RD501/PETP blends was always lower than that predicted by the Maxwell equation (Figs. 7 and 8). The strongest deviation from the Maxwell equation was obtained for the 50/50 blend. It may be suggested on the basis of the rheological data that the phase continuity of the LC polymer increases with increasing LC polymer content and that the model of the system assumed in Eq. (4) may not be valid for the 50/50 blend.

    The film-blown blend specimens showed extensive scattering in
their permeability to oxygen and water vapor (Figs. 9 and 10). The
A950/PETP showed particularly poor barrier properties with no im-
provement for any of the studied blends ($\leq 10\%$ LC polymer). At
low LC polymer contents, the RD501/PETP blends showed a greater
permeability than the PETP. The RD501/PETP blend with 30% of
LC polymer exhibited an oxygen permeability 96% lower than that
of PETP. The decrease in water transmission rate for this particular
specimen was almost as large ($\sim 90\%$). These results may be com-
pared with data for stretch-blow-molded LC polymer/PETP blends
where a decrease of up to a 92% in oxygen permeability was ob-
served for the blend with 30% LC polymer [3]. This result is in accord-
ance with the observations made by SEM (Fig. 3b) that the continuity
of the LC polymer component (fibers and ellipsoidal particles) is
enhanced at the higher LC polymer content.

    Film-blown samples with higher LC polymer contents, $\geq 20\%$ LC
polymer in the A950 series and $\geq 40\%$ LC polymer in the RD501
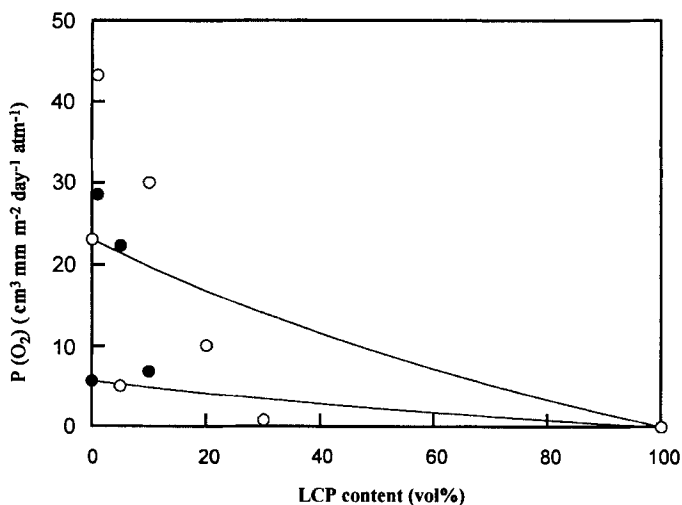series, could not be produced despite several attempts.

FIGURE 9 Oxygen permeability for film-blown A950/PETP ($\bullet$) and RD501/PETP
(O) blends as a function of LC polymer content. The continuous lines are predicted
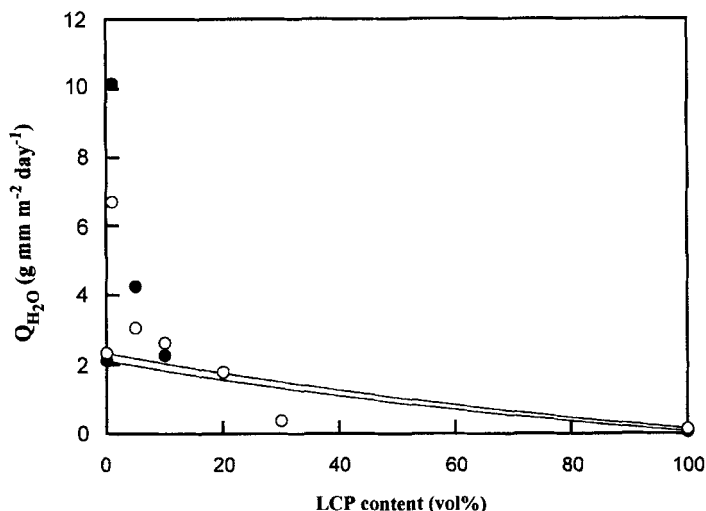values based on Eq. (4).

FIGURE 10   Water vapor transmission rates for film-blown A950/PETP (●) and RD501/PETP (○) blends as a function of LC polymer content. The continuous lines are predicted values based on Eq. (4).

Optical Properties and Seal Strength

Milkiness appeared in the compression-molded blends already with 1% of added LC polymer. The blends turned yellow with a further increase in LC polymer content. The 50/50 blends were beige in color. The uniform color of the blends containing ≤ 30% LC polymer indicated a uniform distribution of LC polymer within each blend. The 50/50 blends showed a coarser texture. A maximum in light absorption was observed between 10 and 50% LC polymer for RD501/PETP (Fig. 11). A distance (L_{nt}) was defined as the sample-to-object distance where a certain object become totally invisible as viewed through the sample and Figure 12 indicates that the transparency was lost more rapidly in the A950/PETP blends than in the RD501/PETP blends. The film-blown samples were optically clear up to 1% A950 and up to 5% RD501. At higher LC polymer contents, milkiness was observed and at the highest LC polymer content the samples were beige in color.

The seal strength for A950/PETP blends reached a maximum at 5% LC polymer content (Fig. 13). PETP and the blend with 1% of LC polymer showed delamination of the seal during the tensile testing.
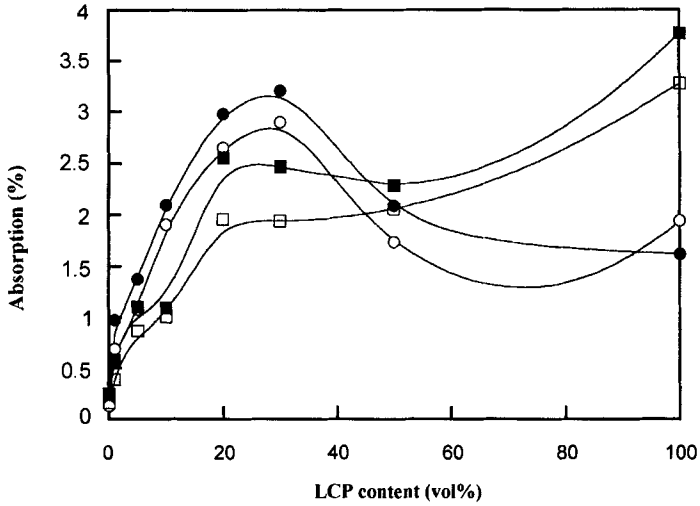
FIGURE 11   Light absorption for compression-molded specimens: RD501/PETP: (●)
$\lambda = 400$ nm, (○) $\lambda = 600$ nm; A950/PETP: (■) $\lambda = 400$ nm, (□) $\lambda = 600$ nm.
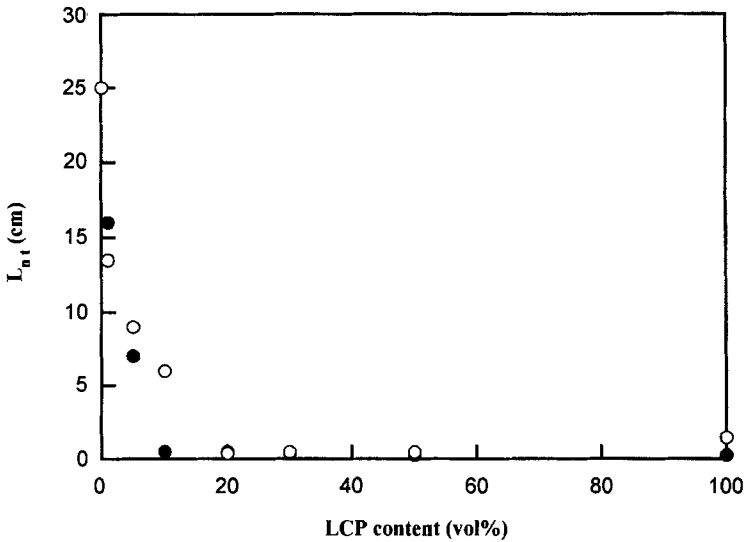

FIGURE 12 L_{nt} as a function of LC polymer content for the compression-molded
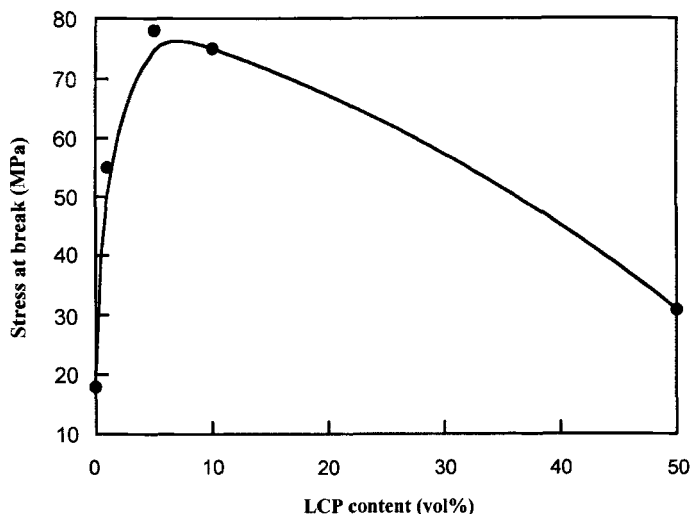A950/PETP (●) and RD501/PETP (○).

FIGURE 13   Stress at break for A950/PETP specimens containing a weld as a function of LC polymer content.

Blends with higher contents of LC polymer showed fractures that were initiated at the thinnest part of the seal and propagated through the material, sometimes accompanied by delamination. Figure 13 shows that the poor sealing properties of PETP may be enhanced by the addition of LC polymer. The drop in seal strength for the 50/50 blend was due to the inherent brittleness of this material. Overall, the seal strength of the LCP/PETP blends was higher than that of the LCP/PE blends [6]. Whereas LCP was detrimental to the seal strength of LCP/PE blends [6], it increased the seal strength of PETP.

CONCLUSIONS

Compression-molded LC polymer/PETP blends consisted of LC polymer spheres in a PETP matrix and the permeability of the blends based on the high melting point Vectra grade could be adequately described with the Maxwell equation, assuming the existance of low permeability (LC polymer) spheres in a high permeability (PETP)

matrix. The compression-molded blends based on the low melting point Vectra grade showed considerably lower permeabilities than were predicted by the Maxwell equation, particularly at high LC polymer contents. Ellipsoidal and fiber-like LC polymer particles were observed at high LCP contents in the film blown systems and they led to a 96% decrease in oxygen permeability compared with that of PETP in the blend based on low melting point Vectra at 30% LC polymer. LC polymer never formed a continuous component in the PETP matrix or at the surface, because the LC polymer had a higher viscosity than PETP. Transparency of the compression-molded samples was lost already at 1% LC polymer. It was found that the blends had superior seal properties than PETP. Finally, it can be stated that the low shear viscosity of the PETP component favors the formation of a discrete LC polymer phase, which is an unsuitable morphology for obtaining superior barrier properties in a blend.

Acknowledgements

References

[1] Day, B. P. F., *Foods and Packaging Materials – Chemical Interactions* (The Royal Society of Chemistry, Cambridge, 1995), Eds. Ackermann, P., Jägerstad, M. and Ohlson, T.
[2] Stöllman, U., *Foods and Packaging Materials – Chemical Interactions* (The Royal Society of Chemistry, Cambridge, 1995), Eds. Ackermann, P., Jägerstad, M. and Ohlson, T.
[3] Lusignea, R. W. (1998). *Proc. Nova-Pack Europe'98 in Düsseldorf*, Oct. 20–21, p. 295.
[4] Wiberg, G., Hedenqvist, M. S., Boyd, R. H. and Gedde, U. W. (1998). *Polym. Eng. Sci.*, **38**, 1640.
[5] Baird, D. G. and Wilkes, G. L. (1983). *Polym. Eng. Sci.*, **23**, 632.
[6] Flodberg, G., Hedenqvist, M. S., Sadiku, E. R., Hellman, A. and Gedde, U. W. (2000). *Polym. Eng. Sci.*
[7] Flodberg, G., Karlsson, S., Hedenqvist, M. and Gedde, U. W., manuscript.
[8] Paul, D. R. and Barlow, J. W. (1980). *J. Macromol. Sci., Rev. Macromol. Chem.*, **C18**, 109.
[9] Ko, C. U., Wilkes, G. L. and Wong, C. P. (1989). *J. Appl. Polym. Sci.*, **37**, 3063.

[10] Zoller, P. and Bolli, P. (1980). *J. Macromol. Sci.-Phys.*, **B18**, 555.
[11] *Vectra A950 Data Sheet*, Ticona (Germany).
[12] Progelhof, P. C., Throne, J. L. and Ruetsch, R. R. (1976). *Polym. Eng. Sci.*, **16**, 615.
[13] Hedenqvist, M. and Gedde, U. W. (1996). *Progr. Polym. Sci.*, **21**, 299.